Matsar: A Comprehensive Machine Learning Approach for Polsar Data Processing

Samay Shetty
Rochester Institute of Technology
Rochester, New York
United States, 14623

SayanPanja
Vidyalankar Institute of Technology
Wadala, Mumbai
India

Jose Akkarapatty
Vidyalankar Institute of Technology
Wadala, Mumbai
India

Soham Pal
Vidyalankar Institute of Technology
Wadala, Mumbai
India

Aarya Shinde
Vidyalankar Institute of Technology
Wadala, Mumbai
India

Avinash Dhiran
Vidyalankar Institute of Technology
Wadala, Mumbai
India

Bhakti Talele
Vidyalankar Institute of Technology
Wadala, Mumbai
India

Sai Gurav
Vidyalankar Institute of Technology
Wadala, Mumbai
India

Varsha Turkar
Vidyalankar Institute of Technology
Wadala, Mumbai
India

Yogesh Agarwadkar
InfiCorridor Solutions PVT LTD
Mumbai, India

Gulab Singh
Indian Institute of Technology – Bombay,
Mumbai, India

ABSTRACT

Polarimetric Synthetic Aperture Radar (PolSAR) data collection has evolved considerably over the years. Access to PolSAR data was initially limited due to its high cost, but now an increasing amount of free data is available, greatly advancing progress in the field. PolSAR, a microwave remote sensing technology, provides invaluable insights into Earth's surface through the analysis of polarimetric properties of radar signals. PolSARPro and SNAP are widely utilized free and open-source software programs developed by the European Space Agency (ESA). They include a few classifiers like Wishart (in PolSARPro), Support Vector Machine (in PolSARPro) and Random Forest (in SNAP). However, these programs have some limitations like they can only apply one classifier at a time for a specific area, and in PolSARPro, classifiers can be applied on coherency [T3] or covariance [C3] matrices, not on stacked decomposed images or various features. Additionally, these software tools do not support parallel computing. To address these issues a new user-friendly GUI-based tool: MATSAR, is proposed to make PolSAR data processing easy for everyone from experienced researchers to novices. By integrating advanced processing capabilities with an intuitive interface, MATSAR aims to facilitate broader and more effective utilization of PolSAR data, offering a solution to the current limitations faced in the field.

General Terms

Machine Learning, PolSAR

Keywords

Remote Sensing, PolSAR, Graphical User Interface, Machine Learning, PolSARPro, Parallel Computing

1. INTRODUCTION

Remote sensing remotely collects Earth surface data with airborne or spaceborne sensors and consists of Optical and Microwave Remote Sensing. Microwave Remote Sensing, unlike optical methods, operates in all weather conditions by penetrating dust and clouds. Synthetic Aperture Radar (SAR) produces high-resolution images by simulating a large antenna along its trajectory, while Polarimetric SAR (PolSAR) provides an extension to SAR by transmitting and receiving signals in various polarizations, perceiving more surface characteristics. PolSAR data processing requires special software like PolSARPro and SNAP (ESA), in addition to software like MIDAS (ISRO) and libraries like pyroSar, SARsen, and SARpy for Python. But PolSARPro only supports classification of coherency (T3) and covariance (C3) matrices using Wishart and SVM classifiers only, while SNAP provides more classifiers like Random Forest, KNN, KDTree KNN, Maximum Likelihood, and Spectral Angle Mapper. Machine learning has been utilized by some researchers for PolSAR classification, like Decision Trees, which have been used on SAR data [1][2], and Random Forest [3], which outperformed decision trees for crop identification. Neural networks and fuzzy logic have also been utilized [4][5][6] and SVMs for land cover mapping [7][8]and Fuzzy SVM, an extension of conventional SVM [9] introduced a generalized ML model which avoids feature extraction and is suitable for use in multiple geographic areas. To overcome current limitations, MATSAR is introduced as an advanced classifier tool, which classifies coherency (T3), covariance (C3) matrices, stacked decomposed images, and other characteristics like texture. It offers comparative investigation between decomposition techniques and ML classifiers with hyperparameter tuning. MATSAR can be parallel processed and GPU-accelerated and speeds up the computation to a great extent. With classifiers such as SVM, Random Forest, Decision Tree, and ANN.

2. DATASET AND GROUND TRUTH

The paper utilizes ALOS PALSAR-2 data for Mumbai city. Table 2 details the data specifications. Mumbai is an island connected to Thane district and bordered by the Arabian Sea. The city's elevation ranges from 10 m to 15 m, averaging 14 m, with its northern region reaching up to 450 m in height.

The field work of Mumbai was carried out by authors in May 2024, it shows that there are no major changes in the geographical region of Mumbai as compared to 2015 [10]. This was confirmed by comparing it with the ground truth taken in 2015. Figure 1 shows PauliRGB image obtained from ALOS PALSAR-2 Mumbai image acquired on 5 March 2015 with ground truth information. The PauliRGB images and corresponding photographs taken during the field work along with latitude and longitude are shown in Figure2 Mangroves (Lat 19.23432° Long 72.822409°) are located on the banks of Gorai Creek.

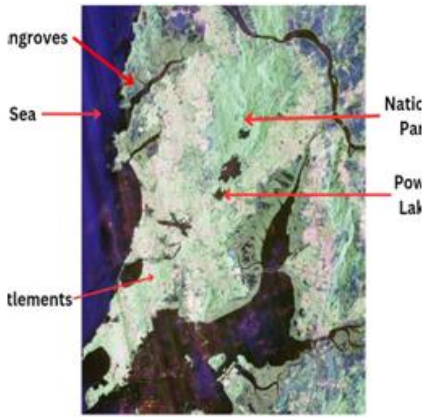

Figure 1: ALOS PALSAR-2 Mumbai image acquired on 5 March 2015 (19.0760° N, 72.8777°E)

Table 1: Current Software in the field of PolSAR Data Processing

SOFTWARE USED FOR PolSAR DATA PROCESSING			
SOFTWARE	FEATURES	ADVANTAGES	LIMITATIONS
PolSARPro	Supports various data formats. (e.g., ALOS, RADARSAT).	Efficient processing for large datasets.	Commercial software with licensing costs. (Lee et.al, 2008)
	Time series analysis capabilities.	Leverages the power of GPUs. (Lee et.al, 2008; Cloude et.al, 2010)	Limited processingcapabilities for non-polarimetric data. (Cloude et.al,2010)
SNAP	User-friendly interface with various plugins.	Open-source and free to use.	May require scripting knowledge for complex workflows.
	Supports multi-mission data.		Limited advanced processing capabilities for polarimetric data.
MIDAS	Extensive visualization and analysis tools.	Flexible and customizable platform for various image processing tasks.	Steeper learning curve compared to user-friendly GUI-based software.
	Supports integration with external software.		Requires programming knowledge for advanced functionalities.

Pyro SAR is an object-oriented Python library designed for intuitive workflows, offering efficient processing for large datasets and leveraging GPU power. However, it requires familiarity with object-oriented programming and has fewer built-in functions compared to SARpy. SARsEN, an open-source and free library, provides a user-friendly interface for common SAR tasks and integrates well with scientific Python libraries. Despite this, it has limited capabilities for advanced polarimetric and interferometric processing and may require coding for complex workflows. SARpy supports various data formats and offers extensive functionalities for SAR processing, but it has a steeper learning curve and can be computationally demanding for complex tasks on limited hardware.

Table 2: Dataset used

Area	Sensor	Date of Acquisition	Band	Polarization	Resolution
Mumbai	ALOS PALSAR-2	05 March 2015	L-Band	Quad	8.7m x 5.3m

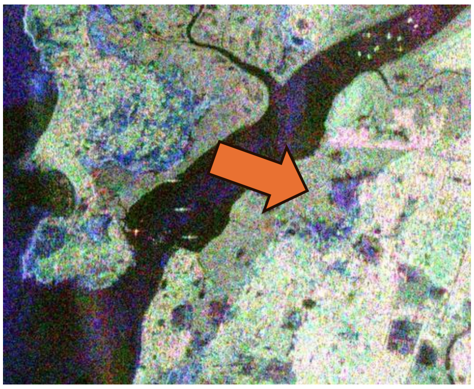

(a) Pauli RGB Image

(b) Photograph During Field Work

Figure2: Mangroves at Gorai Creek (Lat 19.23432° Long 72.822409°)

3. GRAPHICAL USER INTERFACE

As shown in Figure3, the interface includes various buttons, figures, input box and checkboxes. Initially, the user uploads the PolSARPro generated PauliRGB image by clicking on the 'Upload' button. Subsequently, the user is prompted to select the data file and enter the number of classes.

Upon clicking the 'Input' button, a dialog box appears, instructing the user to input the number of training areas and assign a color to each class. Following this, the user can select the option of 'ROI', leading to a pop up of the PauliRGB image for selecting subsequent training areas. The validation button helps the user to select ROI for test accuracy, here the user is also asked by the directory where he would like to save classified image files once all the training and testing ROI is selected. The next step involves choosing classifiers; users can select single or multiple classifiers by checking the corresponding boxes. The results will be displayed adjacent to each other for easier comparison.

For accuracy assessment, two buttons are provided for each training and testing accuracy. Features like Confusion Matrix, Accuracy, Precision, Recall and F1 score are provided. Fig3presents the conceptual framework of the final interface; Fig 4 shows the application interface.

classification techniques without being restricted to a single approach.

Initially, the PolSAR data is processed using PolSARPro, which includes standard preprocessing steps such as calibration, speckle filtering, and matrix generation. In this work, Lee Refined filter (3×3 window) is used to reduce speckle noise and obtain a filtered [T3] coherency matrix, which serves as a fundamental input for further decomposition and classification.

On this filtered [T3] matrix, various decomposition techniques are applied, including:

1. Gulab Singh 4-component (G4U) decomposition
2. Gulab Singh 6-component (6SD) decomposition
3. Gulab Singh 7-component (7SD) decomposition
4. Yamaguchi 3-component decomposition

These decompositions provide insight into different scattering mechanisms and improve the feature representation of the data. The output files of these decompositions, along with the filtered [T3] matrix and the corresponding PauliRGBimage, are saved in .bin format for further processing and classification. The PauliRGB image is particularly useful for visually inspecting the scene and selecting Regions of Interest (ROI) for training and validation.

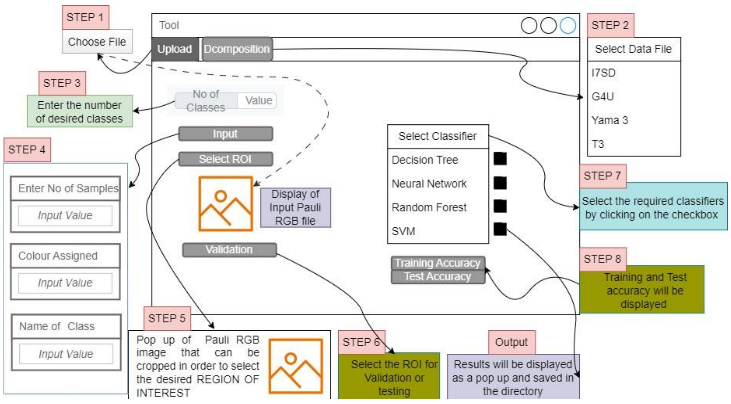

Figure 3: Framework

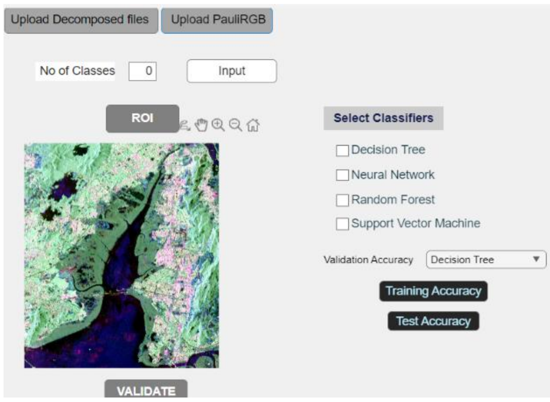

Figure4: Interface

4. METHODOLOGY

The objective of MATSAR is to give users or researchers the option to apply more non-parametric classifiers, the ability to classify the decomposed images, and provide comparative analysis—creating an add-on support for PolSARPro and SNAP. This tool is designed to be flexible and accessible, enabling researchers to explore different decomposition and

As illustrated in Figure 5, the workflow of MATSAR begins by uploading the [T3], decomposed files, and PauliRGB image into the GUI. The GUI is designed to be interactive and user-friendly. The PauliRGB image is displayed to assist the user in manually selecting ROIs based on visual interpretation and ground truth knowledge. The user is prompted to specify:

1. The number of classes

2. Number of training areas (ROIs)
3. Name of each class
4. Color code for visualization

The ROI selection is crucial and assumes that the selected region entirely belongs to the respective class, relying on ground truth knowledge or prior information. Once the ROIs are defined, MATSAR extracts the corresponding pixel values from each stacked feature file (e.g., [T3], 6SD, etc.). These values are vertically concatenated and labeled, forming the training dataset in the shape of M × N, where M is the total number of pixels across all ROIs and N is the number of stacked features or channels (e.g., N=9 for [T3], N=7 for 7SD).

For classification, the user can select from a variety of machine learning classifiers implemented in the backend:

1. Decision Tree (DT): Uses the Gini Index as a splitting criterion. The tree has no depth restriction, and pruning is disabled to preserve maximum detail.
2. Random Forest (RF): Implements bagging with 50 trees, also using the Gini Index. This ensemble method helps reduce overfitting and improve generalization.
3. Artificial Neural Network (ANN): A three-layer network (Input–Hidden–Output). The Input layer is dynamically set based on the number of input features. The Hidden layer has 20 neurons with a Log-Sigmoidactivation function, and the Output layer uses a Linear activation function based on the number of classes.
4. Support Vector Machine (SVM): Uses a Radial Basis Function (RBF) kernel and implements the one-vs-one coding scheme for multi-class classification.

Due to the large volume of PolSAR data, training and prediction tasks can be computationally intensive when run sequentially. To address this, MATSAR is designed to leverage parallel computing using a Graphical Processing Unit (GPU). An algorithm detects the availability of a GPU on the host system. If a GPU is present, computations are offloaded to it; otherwise, the application defaults to running on the CPU. GPU acceleration significantly improves the speed of model training, prediction, and post-classification operations such as:

- Color coding of the classified image
- Element-wise operations
- Reshaping and formatting output data for visualization

MATSAR also includes a built-in interface for visual comparison of classifier outputs. Results from different classifiers are displayed side by side, enabling users to interpret and analyze classification performance with ease. Additionally, the application allows flexibility in choosing the classes to be compared, based on user interest.

After classification, accuracy assessment is performed using both training and test regions. Standard metrics such as overall accuracy, per-class accuracy, and confusion matrix are generated to evaluate the performance of the selected classifier. These insights assist users in determining the best-suited classifier and decomposition combination for their specific application or dataset.

This modular, extensible, and user-centric methodology allows MATSAR to serve as a powerful add-on for PolSAR image classification, giving users the freedom to explore, analyze, and compare multiple classification strategies efficiently.

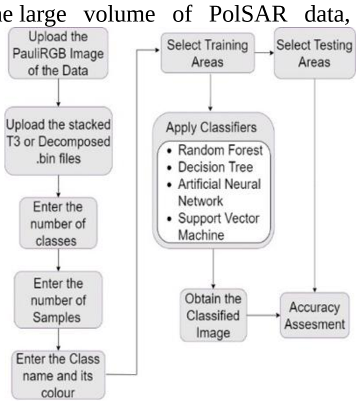

Figure 5: Flowchart for MATSAR

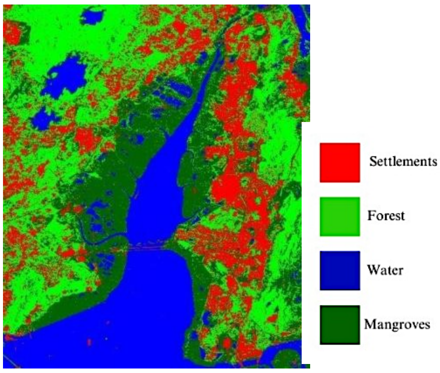

Figure 6: RF Classification (Accuracy 93.73%)

5. RESULTS

Testing has been performed on ALOS PALSAR-2 L-band data of Mumbai. The classification is performed on the subset of Mumbai area for four classes namely settlement (C1), forest (C2), water body (C3) and mangroves (C4). The results are shown as follows for [T3] and various decompositions namely YAMA3, G4U, 6SD and 7SD with classifiers DT, RF, ANN and SVM.

5.1 Coherency Matrix [T3]

The results of the classification applied using RF have been shown in Figure6.Table 3 shows the performance metrics of [T3] when classified using the DT, ANN, RF and SVM classifiers. The highest overall accuracy, 97.90% is achieved when the [T3] is classified using the Random Forest followed by Decision Tree with 96.32%.

Table 3:Performance Metrics

[T3] Matrix					
Classifier	Overall Accuracy (%)	Precision	Recall	F1 Score	Kappa Coefficient
Decision Tree (DT)	93.21	0.994	0.996	0.995	0.992
Artificial Neural Network (ANN)	93.73	0.975	0.965	0.970	0.953
Random Forest (RF)	92.84	0.999	0.999	0.999	0.999
Support Vector Machine (SVM)	87.69	0.983	0.894	0.936	0.965

5.2 Yamaguchi 3-Decomposition

The results of the classification applied using ANN have been shown in Figure7. Table 4: shows the performance metrics of YAMA3 when classified using the DT, ANN, RF and SVM classifiers. The highest overall accuracy, 93.25% is achieved when the YAMA3 decomposed image was classified using the Support Vector Machine followed by Random Forest with 91.40%.

Table 4: Performance Metrics (YAMA3 Decomposition Method)

Classifier	Overall Accuracy (%)	Precision	Recall	F1 Score	Kappa Coefficient
Decision Tree (DT)	93.65	0.977	0.973	0.975	0.976
Artificial Neural Network	93.91	0.936	0.873	0.903	0.912
Random Forest (RF)	92.75	0.844	0.962	0.899	0.894
Support Vector Machine	93.83	0.998	0.998	0.998	0.998

5.3 Gulab Singh 4-Decomposition

The results of the classification applied using RF have been shown in Figure 8. Table 5 shows the performance metrics of G4U decomposed image when classified using DT, ANN, RF and SVM classifiers. The highest overall accuracy, 97.49% is achieved when the G4U decomposed image was classified using the Random Forest followed by Decision Tree with 96.44%.

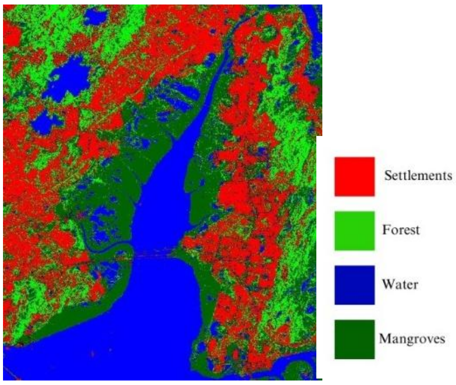

Figure7: ANN Classification (Accuracy 93.91%)

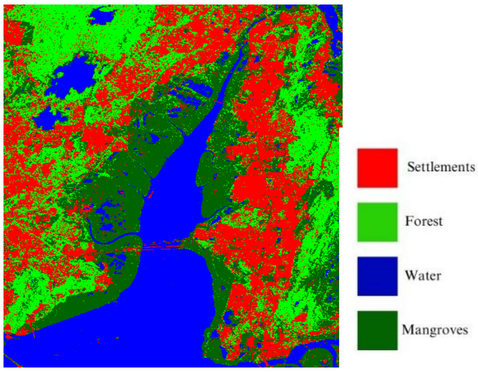

Figure8:RF classification (Accuracy 96.14%)

Table 5: Performance Metrics

G4U Decomposition Method					
Classifier	Overall Accuracy (%)	Precision	Recall	F1 Score	Kappa Coefficient
Decision Tree (DT)	92.29	0.980	0.971	0.975	0.981
Artificial Neural Network (ANN)	92.31	0.972	0.881	0.925	0.943
Random Forest (RF)	96.14	0.882	0.672	0.763	0.889
Support Vector Machine (SVM)	94.87	0.983	0.982	0.983	0.985

5.4 Gulab Singh 6-Decomposition

The results of the classification applied using SVM on 6SD have been shown in Figure9and Table 6 shows the performance metrics of 6SD decomposed image when classified using DT, ANN, RF and SVM classifiers. The highest overall accuracy, 96.52% is achieved when the 6SD decomposed image is classified using the Random Forest followed by Support Vector Machine with 95.74%.

Table 6: Performance Metrics

6SD Decomposition Method					
Classifier	Overall Accuracy (%)	Precision	Recall	F1 Score	Kappa Coefficient
Decision Tree (DT)	95.88	0.999	0.998	0.998	0.994
Artificial Neural Network (ANN)	96.55	0.983	0.978	0.980	0.970
Random Forest (RF)	96.77	0.995	0.996	0.995	0.992
Support Vector Machine (SVM)	97.16	0.996	0.992	0.994	0.971

5.5Gulab Singh 7-Decomposition

The results of the classification applied using SVM on 7SD have been shown in Figure10and Table 7 shows the performance metrics of 7SD decomposed image when classified using DT, ANN, RF and SVM classifiers. The highest overall accuracy, 96.07% is achieved when the 7SD decomposed image was classified using the Random Forest followed by Support Vector Machine with 94.09%.

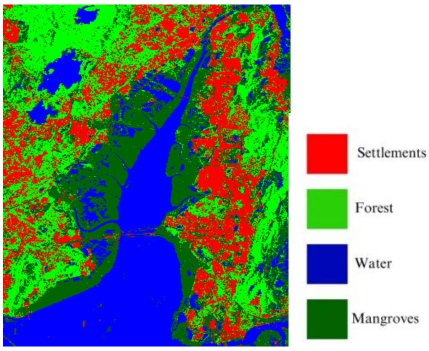

Figure9: SVM Classification (Accuracy 97.16%)

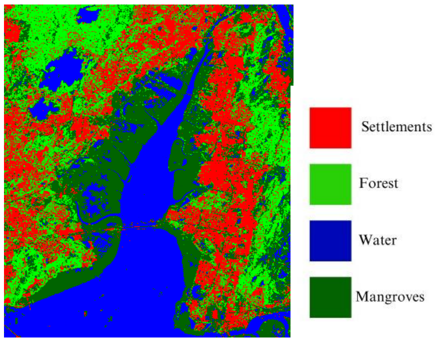

Figure10: SVM Classification (Accuracy 98.05%)

Table 7: Performance Metrics

7SD Decomposition Method					
Classifier	Overall Accuracy (%)	Precision	Recall	F1 Score	Kappa Coefficient
Decision Tree (DT)	95.33	0.983	0.983	0.983	0.983
Artificial Neural Network (ANN)	96.11	0.963	0.848	0.902	0.918
Random Forest (RF)	97.34	0.921	0.888	0.904	0.918
Support Vector Machine (SVM)	98.05	0.992	0.994	0.993	0.994

5.6 Accuracy Analysis

Table 8 (a), (b), (c) and (d) display a comparative study of the test accuracy obtained for Class 1 (Settlements), Class 2 (Forest), Class 3 (Water) and Class 4 (Mangroves) respectively.

Table 9 compares the overall accuracy achieved from these classifiers when implemented on the decomposed images.

Table 8: Test Accuracy (%)

(a) Class 1 – Settlements

CLASSIFIERS	DECOMPOSITION METHODS				
	[T3]	YAMA3	G4U	6SD	7SD
DT	88.96	89.92	84.04	86.02	90.50
ANN	89.53	90.09	84.23	91.19	91.12
RF	74.69	88.63	89.55	88.11	94.72
SVM	77.17	88.97	83.49	88.66	.72

(b) Class 2 – Forest

CLASSIFIERS	DECOMPOSITION METHODS				
	[T3]	YAMA3	G4U	6SD	7SD
DT	90.08	91.17	85.50	97.50	90.83
ANN	91.88	90.09	85.00	95.83	93.33
RF	96.67	92.35	95.00	99.00	94.66
SVM	77.17	92.98	96.00	100	.50

(c) Class 3 – Water

CLASSIFIERS	DECOMPOSITION METHODS				
	[T3]	YAMA3	G4U	6SD	7SD
DT	100	100	100	100	100
ANN	100	100	100	100	100
RF	100	100	100	100	100
SVM	100	100	100	100	100

(d) Class 4 – Mangroves

CLASSIFIERS	DECOMPOSITION METHODS				
	[T3]	YAMA3	G4U	6SD	7SD
DT	93.80	93.5	99.61	97.50	100
ANN	93.51	90.01	100	95.83	100
RF	100	93.27	100	100	100
SVM	100	93.57	100	100	100

Table 9: Overall Accuracy

Overall Accuracy (%)					
CLASSIFIERS	DECOMPOSITION METHODS				
	[T3]	YAMA3	G4U	6SD	7SD
Decision Tree (DT)	93.21	93.65	92.29	95.88	95.33
Artificial Neural Network (ANN)	92.84	93.91	92.31	96.55	96.11
Random Forest (RF)	92.84	92.75	96.14	96.77	97.34
Support Vector Machine (SVM)	87.69	93.83	94.87	97.16	98.05

Table 10:Comparative Analysis of Classification Accuracy (%) for Various Target Decompositions Using Random Forest

CLASSES	DECOMPOSITION METHODS				
	[T3]	YAMA3	G4U	6SD	7SD
Water	100	100	100	100	100
Settlement	77.17	88.97	83.49	88.66	94.72
Forest	77.17	92.98	96.00	100	97.50
Mangroves	100	93.57	100	100	100
Overall Accuracy	87.69	93.83	94.87	97.16	98.05

As shown in Table 8 (a), a 7SD decomposed image when classified using the RF and SVM classifier gives the highest accuracy of 94.72% for settlements. From Table 8 (b), 6SD image when classified using SVM classifier gives the highest accuracy (100%) for forest. It is also observed from Table 8 (c) that the water class gives 100 % accuracy for all the classifiers and decomposition techniques. From Table 8 (d), it is observed that the highest accuracy obtained is 100.00% for Mangroves, when a YAMA3 decomposed image is classified using ANN and SVM classifiers.

As shown in Table 9 7SD gives the highest classification accuracy (98.05%) when classified using SVM, followed by RF classifier (97.34%).The second-highest classification accuracy is achieved by 6SD when classified using SVM (97.16%) followed by RF (96.77%).

Table 10demonstratesthe performance of SVM classifier on different decompositions. It is observed that for all classes except forest 7SD gives the highest accuracy and 6SD gives the highest accuracy for the forest class.

6. CONCLUSION

In conclusion, the development of MATSAR represents a significant advancement in the field of remote sensing. By offering a user-friendly interface and a comprehensive set of classifiers, the tool empowers both novice and expert users to analyze PolSAR data with ease and accuracy. The unique feature of simultaneous application of multiple classifiers enables efficient comparative analysis, facilitating informed decision-making in data interpretation.

MATSAR, offers a user-friendly interface that allows users to choose any input data (such as [T3], [C3], or stacked features) and select one or multiple machine learning algorithms with ease. It also offers flexibility to adjust and fine-tune parameters for training and utilizing machine learning models. Users can apply multiple classifiers simultaneously using this tool on a particular geographical region for same training areas which helps them to do comparative analysis. These experiments have demonstrated the robustness and effectiveness of the tool on ALOS2-PALSAR Mumbai dataset and various classifiers for different target decomposition techniques. The result showsSVM emerging as a standout performer in terms of accuracy. Additionally, the superior performance of 7SD decomposition highlights the versatility of this tool in handling different data processing tasks. The tool's support for parallel computing and the utilization of Graphics Processing Units (GPUs), significantly speeds up the processing time. This provides advantages over other free software available.

The future scope of MATSAR holds promise for further enhancements, including the capability to process raw data formats directly and apply more machine learning classifiers. This development will streamline the data processing workflow and enhance the tool's independence from existing software applications, thereby improving efficiency and usability.

Overall, the machine learning based PolSAR data processing tool represents a valuable contribution to the remote sensing community, paving the way for advanced analysis and interpretation of PolSAR data in various applications ranging from environmental monitoring to disaster management and beyond.

7. REFERENCES

[1] Hess, L., Melack, J., Filoso, S., & Wang, N. Y. (1995). Delineation of inundated area and vegetation along the Amazon floodplain with the SIR-C synthetic aperture radar. *IEEE Transactions on Geoscience and Remote Sensing, 33*(4), 896–904. https://doi.org/10.1109/36.406675

[2] Otukei, J. R., Blaschke, T., Collins, M., &Maghsoudi, Y. (2011). Analysis of ALOS PALSAR and TerraSAR-X data for protected area mapping: A case of the Bwindi Impenetrable National Park-Uganda. *IEEE Transactions on Geoscience and Remote Sensing*, pp. 348–351.

[3] Deschamps, B., McNairn, H., Shang, J., & Jiao, X. (2012). Towards operational radar-only crop type classification: Comparison of a traditional decision tree with a random forest classifier. *Canadian Journal of Remote Sensing, 38*(1), 60–68. https://doi.org/10.5589/m12-012

[4] Hara, Y., Atkins, R., Yueh, S., Shin, R., & Kong, J. (1994). Application of neural networks to radar image classification. *IEEE Transactions on Geoscience and Remote Sensing, 32*(1), 100–109. https://doi.org/10.1109/36.285193

[5] Chen, K. S., Huang, W. P., Tsay, D. H., & Amar, F. (1996). Classification of multifrequency polarimetric SAR imagery using a dynamic learning neural network. *IEEE Transactions on Geoscience and Remote Sensing, 34*(3), 814–820. https://doi.org/10.1109/36.499786

[6] Hellmann, M., Jager, G., Kratzschmar, E., &Habermeyer, M. (1999). Classification of full polarimetric SAR-Data using artificial neural networks and fuzzy algorithms. *IEEE Geoscience and Remote Sensing Symposium (IGARSS'09), 4*, 1995–1997.

[7] Fukuda, S., Katagiri, R., &Hirosawa, H. (2002). Unsupervised approach for polarimetric SAR image classification using support vector machines. *IEEE IGARSS'02*, 5, 2599–2601.

[8] Wu, Y., &Vapnik, V. N. (1999). *Statistical learning theory*. *Technometrics, 41*(4), 377. https://doi.org/10.2307/1271368

[9] Turkar, V., Masurkar, A., Das, A., &Daruwala, R. (2023). Development of Generalized Machine Learning Model to Classify PolSAR Data. *IGARSS 2023 - IEEE International Geoscience and RemoteSensingSymposium*. https://doi.org/10.1109/igarss52108.2023.10281706.

[10] Turkar, V., Checker, J., De, S., & Singh, G. (2022). Impact of G4U and 7-component target decomposition on PolSAR image semantic segmentation. *Advances in Space Research, 70*(12), 3798–3810. https://doi.org/10.1016/j.asr.2022.05.034